

Generalized cascaded model to assess noise transfer in scintillator-based x-ray imaging detectors

Ho Kyung Kim^{a)}

School of Mechanical Engineering, Pusan National University, Jangjeon-dong, Geumjeong-gu, Busan 609-735, Korea

(Received 25 May 2006; accepted 18 October 2006; published online 5 December 2006)

For a scintillator-based x-ray imaging detector, the conventional cascaded model is generalized to describe the direct x-ray induced quantum noise. The direct x rays are those that are unattenuated from a scintillator and that directly interact with photosensitive elements. The developed model is applied for an analysis of a photodiode array in conjunction with a phosphor screen and shows a good agreement with the measured noise-power spectrum. © 2006 American Institute of Physics. [DOI: 10.1063/1.2398926]

For a better design and assessment of x-ray imaging systems, linear-systems transfer theory is widely applied as it can represent a complex imaging system as a cascade of simple elementary processes, such as quantum amplification, binomial selection, deterministic blur, and quantum scatter. It therefore describes signal and noise transfer characteristics.¹ Various scintillator-based detectors have been evaluated with this Fourier-based linear-systems approach.^{1,2} Since normally a scintillator has a finite thickness, the quantum detection efficiency is not always perfect. Instead, direct interactions of x rays transmitted through the scintillator within the subsequently located photosensitive elements, for example, photodiode array, may occur. Although these interactions are important signal and noise sources, there has been no sufficient attention paid to the conventional cascaded model analysis. In this study, to consider the direct x-ray induced noise, the cascaded model is generalized by incorporating an additional parallel cascading path for the signal and noise transfers due to the direct x rays. The theoretical framework is based on the parallel-cascade approach,³ which successfully demonstrated the effect of characteristic x-ray reabsorption in a radiographic screen.

The conventional cascaded model for the analysis of a scintillator-based x-ray imaging detector can be described by a number of elementary processes from the incident x-ray fluence \bar{q}_0 to the addition of electronic noise σ_{add} through the paths A, B, and C, as shown in Fig. 1, designated by the solid lines. When \bar{q}_0 interacts in a scintillator with a probability of α (or quantum detection efficiency), path A describes a conversion process of the absorbed energy within the scintillator into the generation of optical photons,² while path B describes a conversion process when a characteristic x ray is produced.³ Path C represents the generation of optical photons remotely due to the reabsorption of the characteristic x rays.³ ω_K and f_K quantify the probabilities that a characteristic x ray will be produced and reabsorbed, respectively. A detailed description of the physical parameters used in this model is summarized in Table I. Noise transfers along each path prior to node 1 can be expressed as

$$\text{NPS}_{1A}(u, v) = \bar{q}_0 \alpha (1 - \omega_K) \frac{\bar{m}_A^2}{I_A}, \quad (1)$$

$$\text{NPS}_{1B}(u, v) = \bar{q}_0 \alpha \omega_K \frac{\bar{m}_B^2}{I_B}, \quad (2)$$

$$\text{NPS}_{1C}(u, v) = \bar{q}_0 \alpha \omega_K f_K \frac{\bar{m}_C^2}{I_C}, \quad (3)$$

where u and v are the spatial-frequency conjugates to x and y in the Cartesian coordinates, respectively. \bar{m}_j is the mean number of secondary quanta and I_j is the statistical or Swank factor corresponding to each amplification process along path j . As the branching between paths A and B is represented as a Bernoulli branch and the input quanta are statistically uncorrelated, the cross spectral density is $\text{NPS}_{1AB}(u, v) = \text{NPS}_{1BA}(u, v) = 0$. Similarly, $\text{NPS}_{1AC}(u, v) = \text{NPS}_{1CA}(u, v) = 0$. In contrast, the branching between paths B and C is a point selection process for identical input quanta, and the cross spectral density is therefore given by³

$$\text{NPS}_{1BC}(u, v) = \text{NPS}_{1CB}(u, v) = \bar{q}_0 \alpha \omega_K f_K \bar{m}_B \bar{m}_C T_K(u, v). \quad (4)$$

These noise spectra are transferred towards node 2 by experiencing successive elementary processes such as an optical quantum scattering in the scintillator and a conversion into the electronic signal charges in a readout-pixel photodiode. Referring to the formalism described in a previous work,⁴ the resultant noise-power spectrum (NPS) prior to node 2 is

$$\text{NPS}_{20}(u, v) = \bar{q}_0 \alpha \bar{m}_1 \eta [1 + \eta M_K(u, v) T_{\text{scn}}^2(u, v)], \quad (5)$$

where

$$\bar{m}_1 = (1 - \omega_K) \bar{m}_A + \omega_K \bar{m}_B + \omega_K f_K \bar{m}_C, \quad (6)$$

^{a)}Electronic mail: hokyung@pusan.ac.kr

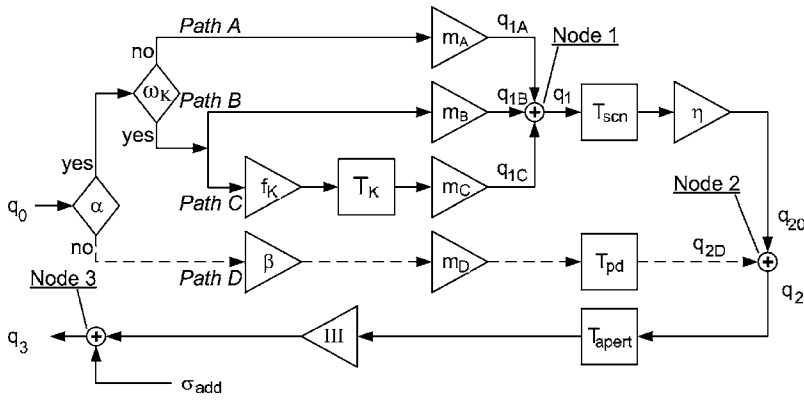


FIG. 1. Block diagram describing the generalized cascaded model to assess the signal and noise transfer in a scintillator-based x-ray imaging detector. Path A describes the conversion of the absorbed energy within the scintillator into the generation of optical photons, while path B describes the conversion process of the absorbed energy when a characteristic x ray is produced. Path C represents the generation of optical photons due to the reabsorption of the characteristic x rays. Path D describes the conversion process of the absorbed energy within a photodiode from direct x rays transmitted through a scintillator into the generation of electronic charges. A detailed description of the physical parameters used in this model is summarized in Table I.

$$M_K(u, v) = \frac{(1 - \omega_K) \bar{m}_A (\bar{m}_A / I_A - 1) + \omega_K \bar{m}_B (\bar{m}_B / I_B - 1) + \omega_K f_K \bar{m}_C (\bar{m}_C / I_C - 1) + 2 \omega_K f_K \bar{m}_B \bar{m}_C T_K(u, v)}{(1 - \omega_K) \bar{m}_A + \omega_K \bar{m}_B + \omega_K f_K \bar{m}_C}. \quad (7)$$

If $\omega_K=0$, i.e., if no characteristic x rays are produced, Eq. (5) is simplified to

$$\text{NPS}_{20}(u, v) = \bar{q}_0 \alpha \bar{m}_A \eta \left[1 + \eta \left(\frac{\bar{m}_A}{I_A} - 1 \right) T_{\text{scn}}^2(u, v) \right], \quad (8)$$

which was widely used for the analysis of an x-ray imaging detector before the parallel model considering the reabsorption of characteristic radiation was introduced.²

Accounting for the direct interaction of x rays transmitted through a scintillator within the photodiode array, an additional *parallel* cascading path D designated by broken lines is incorporated, as shown in Fig. 1. For a selected quantum by the probability of $1 - \alpha$, the additional path successively describes the selection of quanta that interact in the photodiode, the conversion into electronic charges, and the electronic-charge spreading due to the spatial distribution of energy absorption in the photodiode. The splitting of path D from the conventional model follows the Bernoulli branch so

that the cross spectral densities with the other paths are zero. Therefore, entering NPS to node 2 gives

$$\text{NPS}_{2D}(u, v) = \bar{q}_0 (1 - \alpha) \beta \bar{m}_D \left[1 + \left(\frac{\bar{m}_D}{I_D} - 1 \right) T_{\text{pd}}^2(u, v) \right], \quad (9)$$

and the total NPS at node 2 is therefore given by $\text{NPS}_2(u, v) = \text{NPS}_{20}(u, v) + \text{NPS}_{2D}(u, v)$. The NPS at node 2 is then transferred towards node 3 through the two additional processes of the aperture integration and sampling. The model finally employs the addition of electronic noise at node 3. Assuming a squared pixel geometry with a pitch of d and an aperture size in one direction of a , the resultant NPS at node 3 can be expressed by

TABLE I. Summary of the physical parameters used in the generalized cascaded model analysis. Values were computed for a CMOS photodiode array in conjunction with a LanexTM Min-R screen.

Parameters	Description	Values
a	Pixel aperture	0.044 721 mm
d	Pixel pitch	0.048 mm
\bar{q}_0	Incident x-ray fluence	$2.31 \times 10^6 \text{ mm}^{-2}$
α	X-ray detection efficiency in the scintillator	0.48
β	Direct x-ray detection efficiency in the photodiode	1.63×10^{-3}
η	Optical quantum efficiency in the photodiode	0.55
ω_K	Probability that a characteristic x-ray is produced	...
f_K	Probability that a characteristic x-ray is reabsorbed	...
\bar{m}_j	Mean number of secondary quanta at each path j	$\bar{m}_A=635, \bar{m}_D=3072$
I_j	Statistical factor corresponding to each process \bar{m}_j	$I_A=0.66, I_D=0.63$
$T_K(u)$	MTF due to the characteristic x-ray reabsorption	...
$T_{\text{scn}}(u)$	MTF of the scintillator	$(1 + 0.059 96u^2)^{-1}$
$T_{\text{pd}}(u)$	MTF due to the absorbed energy distribution in the photodiode by the direct x-ray interaction	1
$T_{\text{apert}}(u)$	MTF due to the aperture integration	$ \text{sinc}(au) $
$\text{III}(u)$	Sampling process	$\sum_{n=0}^{\infty} \delta(u \pm n/d)$
σ_{add}	Additive electronic noise	1100e

$$\begin{aligned}
\text{NPS}_3(u, v) &= \sum_{j=0}^{\infty} \sum_{k=0}^{\infty} a^4 \text{NPS}_{20} \left(u \pm \frac{j}{d}, v \pm \frac{k}{d} \right) T_{\text{apert}}^2 \left(u \pm \frac{j}{d}, v \pm \frac{k}{d} \right) \\
&+ \sum_{j=0}^{\infty} \sum_{k=0}^{\infty} a^4 \text{NPS}_{2D} \left(u \pm \frac{j}{d}, v \pm \frac{k}{d} \right) T_{\text{apert}}^2 \left(u \pm \frac{j}{d}, v \pm \frac{k}{d} \right) \\
&+ \text{NPS}_{\text{add}}(u, v). \quad (10)
\end{aligned}$$

In order to confirm the developed generalized cascaded model, the NPS of a scintillator-coupled photodiode array detector was measured utilizing a 45 kV x-ray spectrum tailored by a 0.5-mm-thick aluminum filter.⁵ The scintillator is a commercial phosphor screen (Min-R™, Eastman Kodak, USA), which is primarily made up of a terbium-doped gadolinium oxysulfide ($\text{Gd}_2\text{O}_2\text{S:Tb}$). As a *K*-shell photoelectric interaction of gadolinium, mainly contributing to the generation of characteristic radiation in the $\text{Gd}_2\text{O}_2\text{S:Tb}$ screen, occurs for an energy of at least 50.24 keV, it can be assumed that no characteristic x rays are produced in this study. The photodiode array made by a complementary metal-oxide semiconductor (CMOS) process (RadEye™, Rad-Icon Imaging Corp., USA) was employed as the optical photon readout device. The detector has a format of 512×1024 pixels with a pitch of 48 μm .

For the analysis of the measured NPS, the theoretical NPS was calculated based on the developed model. The physical parameters describing the signal and noise properties of the $\text{Gd}_2\text{O}_2\text{S:Tb}$ screen and the CMOS photodiode, such as quantum detection efficiencies and statistical factors, were estimated using Monte Carlo codes, MCNPX™ (Version 2.5.0., ORNL, USA) and DETECT2000 (Laval University, Quebec, Canada) for x rays and optical photons, respectively.

For the assessment of $T_{\text{pd}}(u, v)$, the spatial distribution of energy absorption in a pixel of the photodiode was simulated using a similar methodology to that in a previous work,⁶ and which shows that the distribution is very narrow compared with the pixel size. Therefore, the stochastic blurs in path *D* can be neglected, in other words, $T_{\text{pd}}(u, v) = 1$. From Ref. 7,

$$\sum_{n=0}^{\infty} T_{\text{apert}}^2 \left(u \pm \frac{n}{d} \right) = \sum_{n=0}^{\infty} \left[\frac{\sin\{\pi a(u \pm n/d)\}}{\pi a(u \pm n/d)} \right]^2 = \frac{d}{a}. \quad (11)$$

Thus, the second term on the right side of Eq. (10) can be simplified to $a^2 d^2 \bar{q}_0 (1 - \alpha) \beta \bar{m}_D^2 / I_D$, which indicates that the noise transfer along path *D* is white noise in the spatial-frequency domain. In order to assess the additive electronic noise term, it was assumed that the electronic noise in one pixel was not correlated with the noise in other pixels, and the additive NPS was treated as a white noise spectrum with a magnitude of $d^2 \sigma_{\text{add}}^2$, where σ_{add} is the standard deviation of the additive electronic noise.⁸ All of the values used for the theoretical calculations are given in Table I.

A comparison between the measured and theoretical noise-power spectra is shown in Fig. 2. It is noted that the

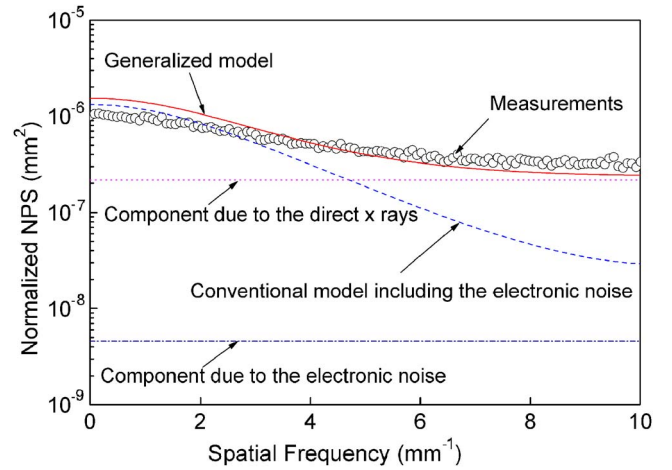


FIG. 2. (Color online) Comparison between the measured and calculated normalized noise-power spectra. While the conventional cascaded model shows a large discrepancy in high spatial-frequency region with the measured data, the generalized model shows a good agreement.

spectra are normalized for the system gain. While the conventional cascaded model shows a large discrepancy with the measured data, the generalized model shows a good agreement. Although the interaction probability of direct x rays transmitted through a scintillator with the photodiode is low, the amplification factor for the generation of secondary quanta is relatively higher due to the lower value of the effective *W* value. If the spreading of secondary quanta is confined in a pixel, this type of noise contributes uniformly in all of the spatial frequencies. Therefore, the noise due to the direct x rays should be considered in a Fourier-based linear-systems analysis for high-resolution imaging systems incorporating a thin scintillator.

In summary, a generalized cascaded model that assesses noise transfer in a scintillator-based x-ray detector has been developed. The developed model provides a good accounting of the contribution of the unattenuated x rays in the image quality. It is useful for the design and assessment of x-ray imaging systems incorporating scintillators as an x-ray converter.

This work was supported by Grant No. R01-2006-000-10233-0 from the Basic Research Program of the Korea Science and Engineering Foundation.

¹M. Sattarivand and I. A. Cunningham, IEEE Trans. Med. Imaging **24**, 211 (2005), and references therein.

²J. H. Siewerdsen, L. E. Antonuk, Y. El-Mohri, J. Yorkston, W. Huang, and I. A. Cunningham, Med. Phys. **25**, 614 (1998).

³J. Yao and I. A. Cunningham, Med. Phys. **28**, 2020 (2001).

⁴S. Richard, J. H. Siewerdsen, D. A. Jaffray, D. J. Moseley, and B. Bakhtiar, Med. Phys. **32**, 1397 (2005).

⁵M. K. Cho, H. K. Kim, T. Graeve, and J.-M. Kim, Key Eng. Mater. **321–323**, 1052 (2006).

⁶H. K. Kim, G. Cho, Y. H. Chung, H. K. Lee, and S. C. Yoon, Nucl. Instrum. Methods Phys. Res. A **422**, 713 (1999).

⁷W. Zhao and J. A. Rowlands, Med. Phys. **24**, 1819 (1997).

⁸H. K. Kim, S. C. Lee, M. H. Cho, S. Y. Lee, and G. Cho, IEEE Trans. Nucl. Sci. **52**, 193 (2005).